J. Mex. Chem. Soc. **2020**, *64*(4)
Regular Issue

ISSN-e 2594-0317

Chemical Constituents from *Artemisia annua* and *Vitex agnus-castus* as New Aromatase Inhibitors: *In-vitro* and *In-silico* Studies

Hend M. Dawood*, Eman Shawky, Hala M. Hammoda, Aly M. Metwally, Reham S. Ibrahim

Department of Pharmacognosy, Faculty of Pharmacy, Alexandria University, Egypt.

***Corresponding author:** Hend M. Dawood, email: henddawoodpharm@hotmail.com

Received June 13th, 2020; Accepted September 24th , 2020.

DOI for main article: http://dx.doi.org/10.29356/jmcs.v64i4.1236

Supplementary Information

J. Mex. Chem. Soc. **2020**, *64*(4)
Regular Issue

ISSN-e 2594-0317

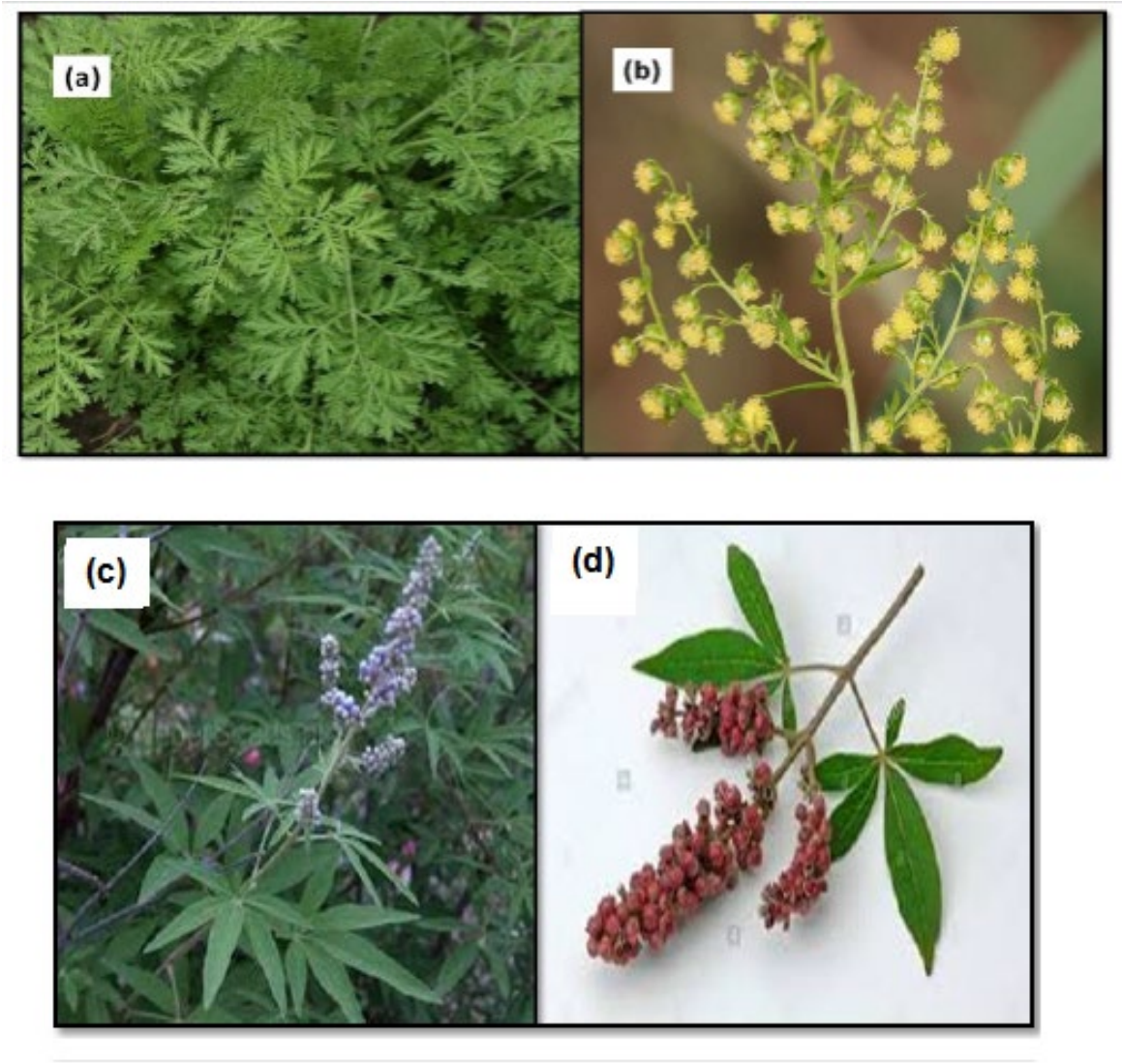

Fig. S1. *Artemisia annua* (**a**) aerial parts and (**b**) inflorescence. *Vitex agnus castus* (**c**) leaves, flowers and (**d**) ripe fruits.

J. Mex. Chem. Soc. **2020**, *64*(4)
Regular Issue

ISSN-e 2594-0317

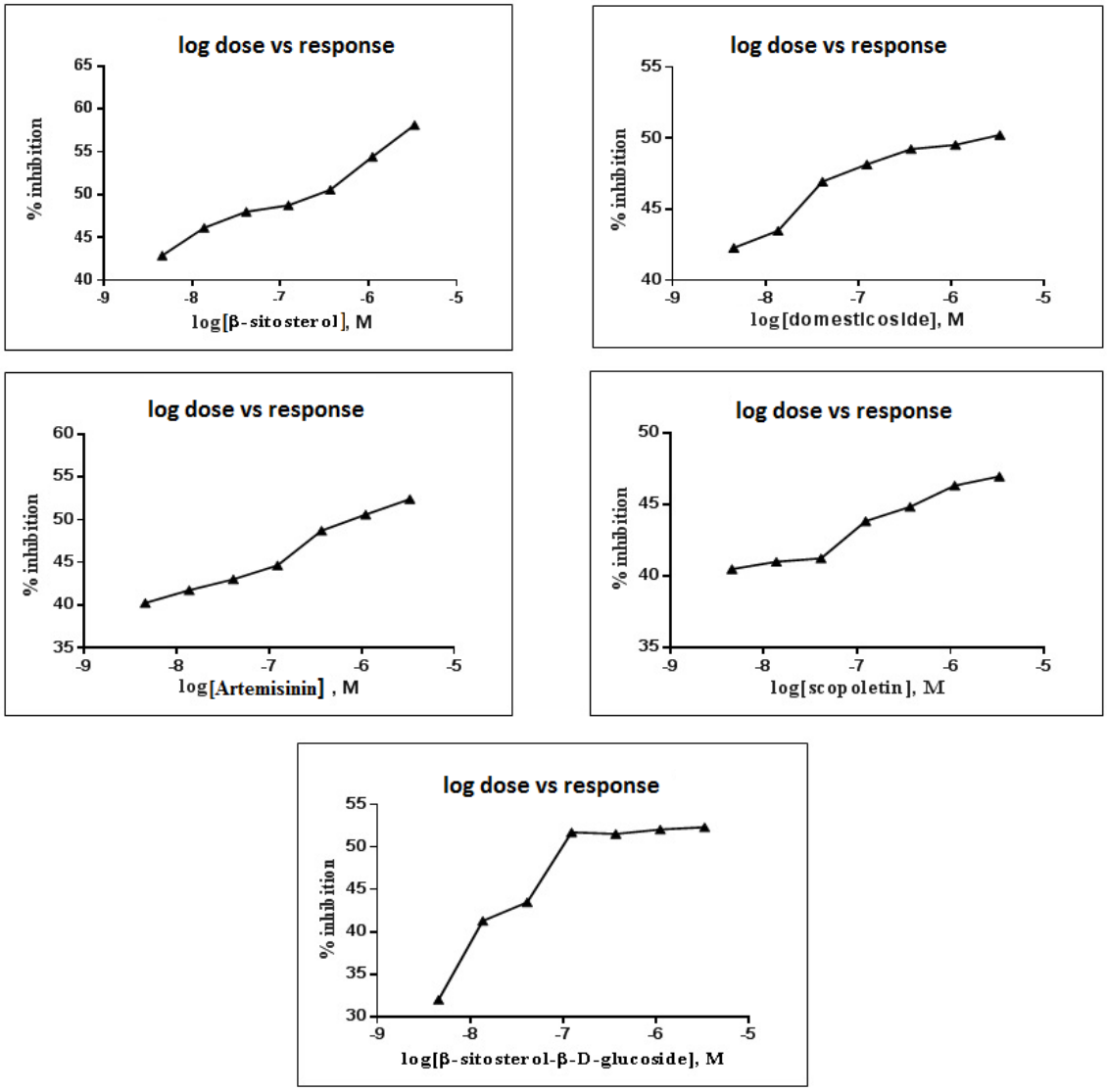

Fig. S2. Dose-response curves for aromatase inhibition by the tested compounds *β*-sitosterol, domesticoside, artemisinin, scopoletin and *β*-sitosterol-*β*-D-glucoside obtained by non-linear regression analysis.

J. Mex. Chem. Soc. **2020**, *64*(4)
Regular Issue

ISSN-e 2594-0317

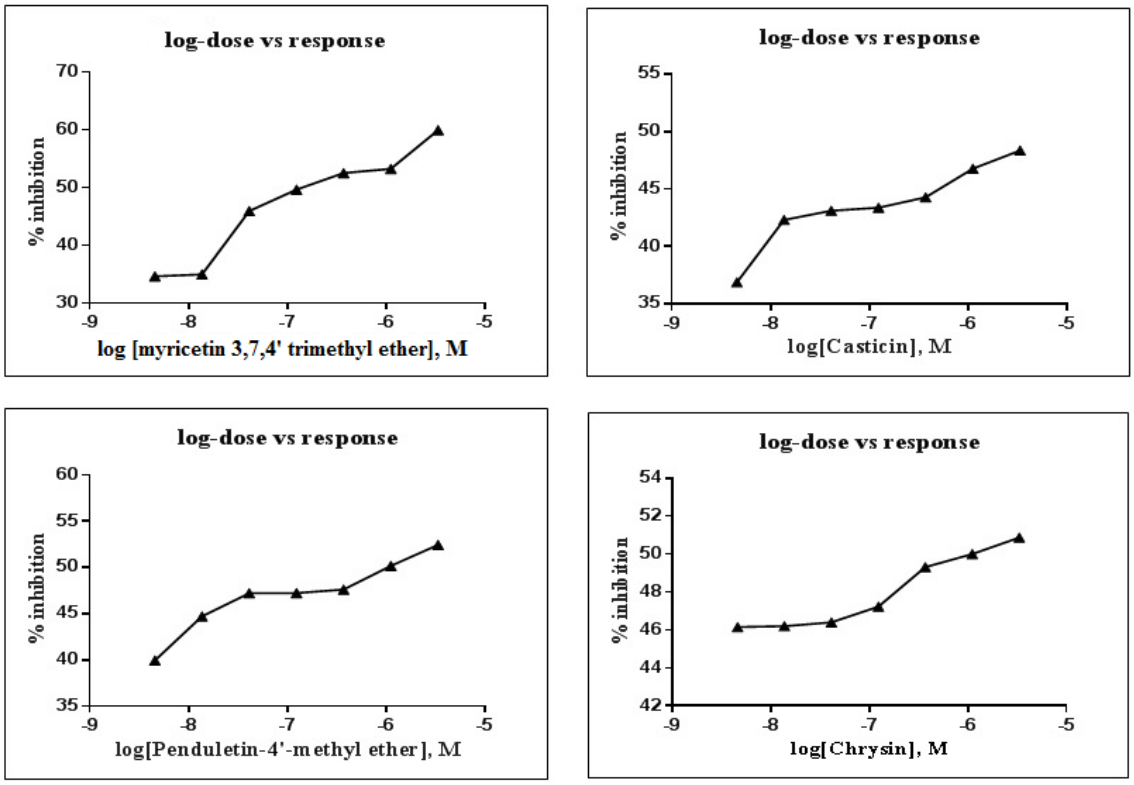

Fig. S3. Dose-response curves for aromatase inhibition by the tested flavonoids and the positive control chrysin obtained by non-linear regression analysis.

J. Mex. Chem. Soc. **2020**, *64*(4)
Regular Issue

ISSN-e 2594-0317

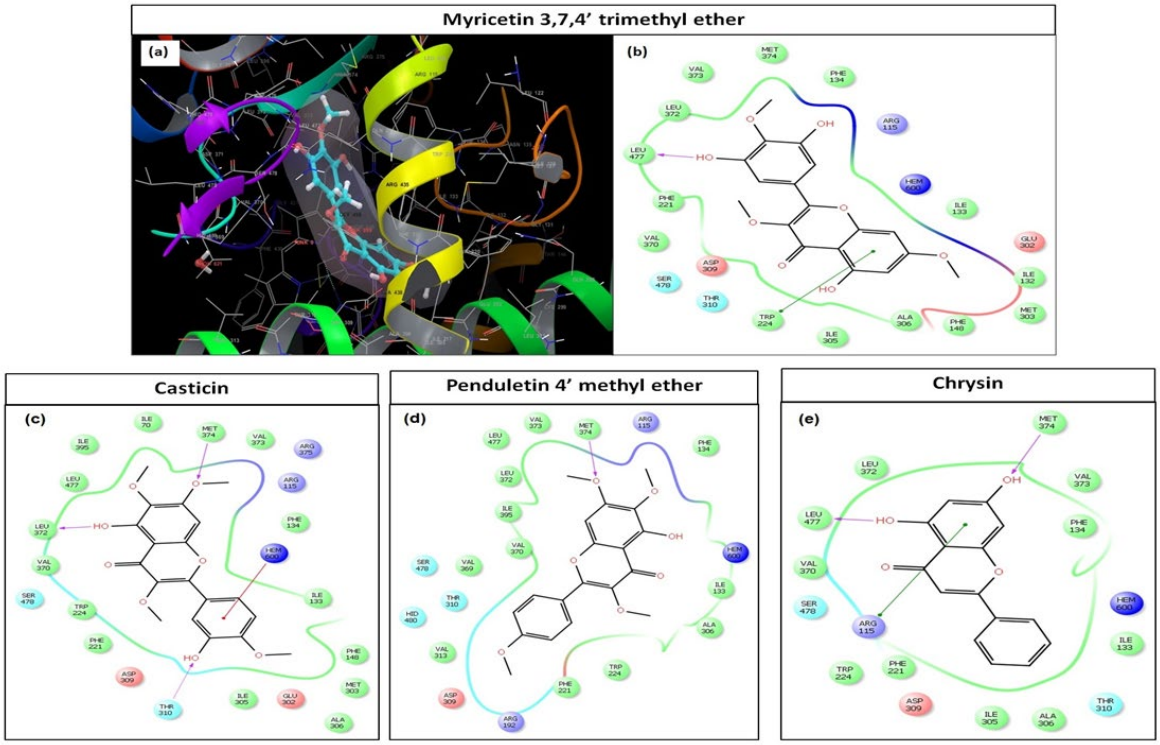

Fig. S4. (**a**) 2D and (**b**) 3D ligand interaction diagrams for docking poses of myricetin-3,7,4'-trimethyl ether in the active site of aromatase crystalline structure (3EQM) together with the 2D interaction diagrams of (**c**) casticin, (**d**) penduletin-4'-methyl ether compared to that of (**e**) chrysin.

J. Mex. Chem. Soc. **2020**, *64*(4)
Regular Issue

ISSN-e 2594-0317

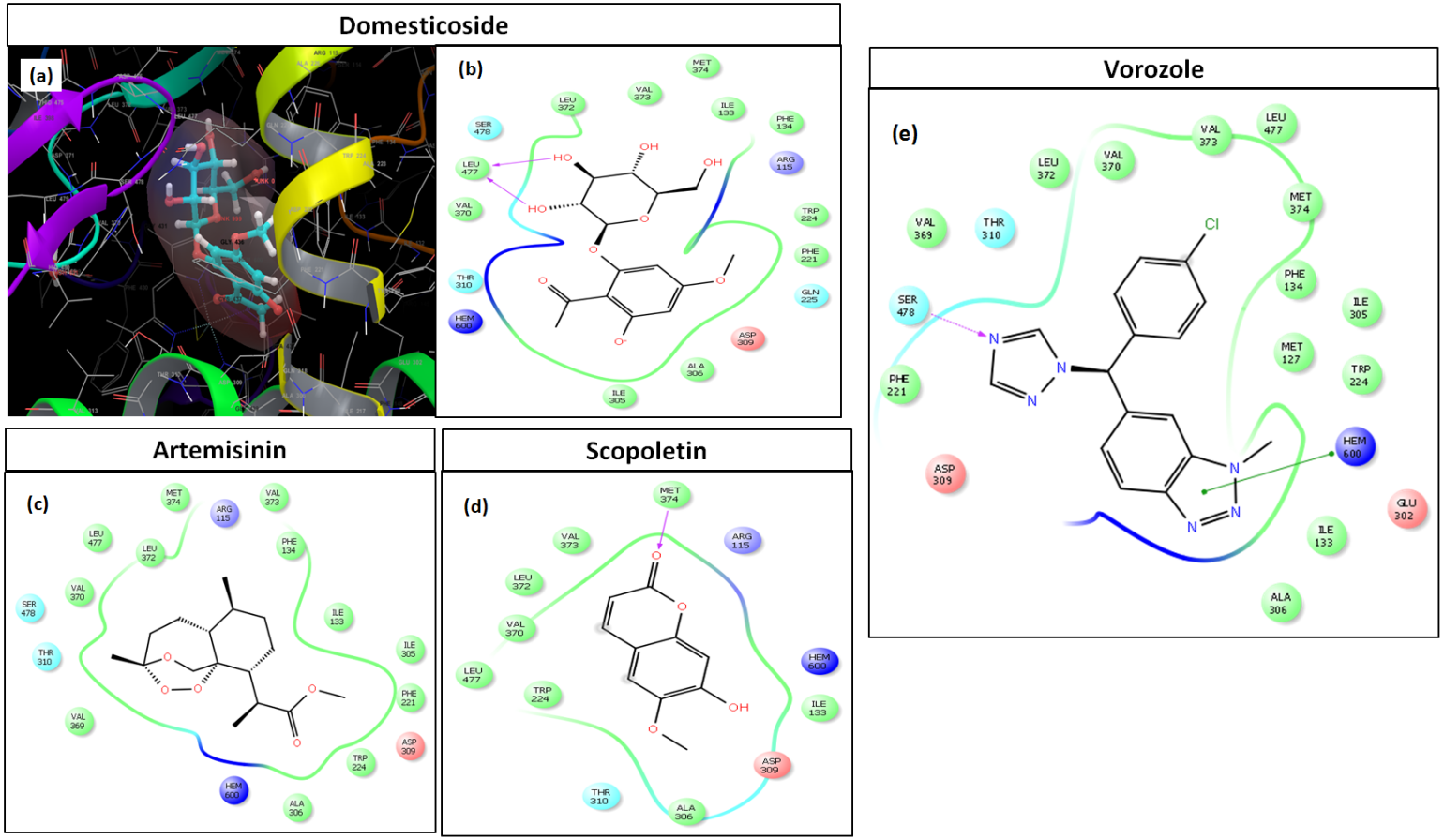

Fig. S5. (a) 2D and **(b)** 3D ligand interaction diagrams for docking poses of domesticoside in the active site of aromatase crystalline structure (3EQM) together with the 2D interaction diagrams of **(c)** artemisinin, **(d)** scopoletin and **(e)** vorozole.

J. Mex. Chem. Soc. **2020**, *64*(4)
Regular Issue

ISSN-e 2594-0317

Table S1. NMR spectral data of Artemisinin.

#	**^{1}H-NMR, δH (400 MHz)**	**APT, δC (100 MHz)**
3	----------	105.40
4*α*(ax) **4*β*(eq)**	2.47 (ddd, 1H, $J_{4\alpha,\ 4\beta}$ = 14.4 , $J_{4\alpha,\ 5}$ = 10.8 , $J_{4\alpha,\ 5a}$ = 3.6 Hz) 2.10 (dd, 1H, $J_{4\beta,\ 4\alpha}$ = 14.4, $J_{4\beta,\ 5}$ = 4.2 Hz)	35.92
5	2.05 (m, 2H, $J_{5\ ,4\alpha}$ = 10.8, $J_{5,\ 5a}$ =10.4, $J_{5,\ 4\beta}$ = 4.2 Hz)	24.80
5a	1.39 (m, 1H, $J_{5a,6}$ = 12.6, $J_{5a,5}$ =10.4, $J_{5a,\ 4\alpha}$ = 3.6 Hz)	50.00
6*β*	1.42 (m, 1H, $J_{6\beta\ ,\ 7}$ = 13.5, $J_{6,5a}$ = 12.6, $J_{6\beta,\ 14Me}$ = 6.0 Hz)	37.50
7	1.82 (m, 2H, $J_{7,\ 6\beta}$ =13.5, $J_{7,8\beta}$ = 11.5 Hz)	23.42
8*α*(eq) **8*β*(ax)**	1.90 (m,1H, $J_{8\alpha,\ 8\beta}$ = 13.3 Hz) 1.10 (m, 1H, $J_{8\beta,\ 8\alpha}$ = 13.3, $J_{8\beta,8a}$ = 12.0, $J_{8\beta,7}$ 11.5 Hz)	33.60
8a	1.76 (m, 1H, $J_{8a,8\beta}$ = 12.0, $J_{8a,\ 9}$ =5.2 Hz)	44.90
9	3.40 (m, 1H, $J_{9,\ 15Me}$ = 7.2, $J_{9,8a}$ = 5.2 Hz)	32.90
10	----------	171.00
12	5.80 (s, 1H)	93.70
12a	----------	79.00
13-Me	1.45 (s, 3H)	25.21
14-Me	1.02 (d,3H, $J_{14Me,\ 6\beta}$ = 6.0 Hz)	19.80
15-Me	1.22 (d,3H, $J_{15Me,\ 9}$ = 7.2 Hz)	12.57

Table S2. NMR spectral data of scopoletin.

#	**^{1}H-NMR, δH (400 MHz)**	**APT, δC (100 MHz)**
1	----------	161.14
2	6.21 (d,1H, $J_{2,3}$= 8 Hz)	112.09
3	7.90 (d,1H, $J_{3,2}$ = 8 Hz)	144.90
4	----------	110.96
5	7.20 (s,1H)	110.10
6	----------	145.70
7	----------	151.64
8	6.78 (s, 1H)	103.21
9	----------	149.98
6-OCH_3	3.82 (s, 3H)	56.45

J. Mex. Chem. Soc. **2020**, *64*(4)
Regular Issue

ISSN-e 2594-0317

Table S3. NMR spectral data of Myricetin 3,7,4' trimethyl ether, penduletin-4'- methyl ether and casticin.

	Myricetin -3,7,4' trimethyl ether		**Penduletin -4'- methyl ether**		**Casticin**	
	^{1}H-NMR, δH (400 MHz)	**APT, δC (100 MHz)**	**^{1}H-NMR, δH (400 MHz)**	**APT, δC (100 MHz)**	**^{1}H-NMR, δH (400 MHz)**	**APT, δC (100 MHz)**
2	----------	156.2	---------	152.79	----------	152.34
3	----------	139.08	---------	138.87	----------	138.10
4	----------	178.91	---------	178.90	----------	178.89
5	----------	157.85	---------	152.30	----------	152.73
6	6.38 (d,1H, $J_{6,8}$ = 4 Hz)	97.86	---------	130.50	----------	132.20
7	---------	146.37	--------	158.67	---------	158.80
8	6.47 (d,1H, $J_{8,6}$ = 4 Hz)	92.17	6.52 (s)	90.33	6.54 (s)	90.34
9	----------	156.84	---------	155.82	---------	155.60
10	----------	105.90	--------	107.05	-------	106.63
1'	----------	122.5	---------	122.8	---------	125.65
2'	7.72(br s, 2H)	101.04	8.1 (d, 2H, J = 8.4 Hz)	130.16	7.72 (d, 1H, $J_{2',6'}$ = 2Hz)	114.34
6'					7.76 (dd, 1H, $J_{6',5'}$ = 8.4, $J_{6',2'}$= 2 Hz)	121.60
3'	----------	141.87	7.05(d, 2H, J = 8.4 Hz)	114.09	----------	145.57
5'					7.00(d, 1H, $J_{5',6'}$ =8.4 Hz)	110.38
4'	--------	162.2	----------	147.71	----------	148.00
3-OMe	3.82 (s, 3H)	61.85	3.89 (s, 3H)	60.15	3.91 (s, 3H)	60.15
6-OMe	---------	--------	3.92 (s, 3H)	60.89	3.96 (s, 3H)	60.89
7 OMe	3.99 (s, 3H)	56.13	3.95 (s, 3H)	56.32	3.99 (s, 3H)	56.31
4'-OMe	3.89 (s, 3H)	60.19	3.98 (s, 3H)	55.46	4.02 (s, 3H)	56.05

J. Mex. Chem. Soc. **2020**, *64*(4)
Regular Issue

ISSN-e 2594-0317

Table S4. NMR spectral data of domesticoside.

#	**^{1}H-NMR, δH (400 MHz)**	**APT, δC (100 MHz)**
1	----------	106.89
2	----------	163.11
3	6.22 (d, 1H, $J_{3,5}$ = 2 Hz)	92.42
4	----------	165.79
5	6.15 (d, 1H, $J_{5,3}$ = 2 Hz)	96.62
6	----------	164.15
7	----------	203.36
8-Me	2.56 (s, 3H)	33.26
4-OMe	3.87 (s, 3H)	56.53
1'	4.99 (d, 1H, $J_{1',2'}$ = 7.6 Hz)	100.04
2'	3.24 (m, 1H, $J_{2',1'}$ = 7.6 Hz)	73.54
3'	3.41 (m, 1H)	77.74
4'	3.15 (m, 1H, $J_{4',5'}$ = 8.8 Hz)	70.19
5'	3.28 (m, 1H, $J_{5',4'}$ = 8.8 Hz)	77.00
6'a 6'b	3.46 (m, 1H, $J_{6'a,6b'}$ = 6.4 Hz) 3.70 (m, 1H, $J_{6'b,6a'}$ = 6.4 Hz)	61.14

J. Mex. Chem. Soc. **2020**, *64*(4)
Regular Issue

ISSN-e 2594-0317

Table S5. Qikprop calculated ADMET descriptors for the eight isolated compounds with provided cut-off ranges for comparison with 95% known drugs.

name of descriptor	Description	Acceptable range	Notes	Artemisinin	Myrcetin-3,7,4' trimethyl ether	Scopoletin	Domesticoside	Penduletin - 4'-methyl ether	Casticin	*β* -sitosterol	*β* -sitosterol 3- *O*-*β* –D-gluco pyranoside
stars	Number of descriptor values falling outside the recommended values for the 95% known drugs. As the number of stars increases, the molecule is less drug-like.	0-5		1	0	0	0	0	0	6	3
#rtvFG	Number of reactive functional groups leading to false positives in HTS assays	0 – 2		4	0	1	1	0	0	0	1
mol_MW	Molecular weight of the molecule	130 – 725		282.336	360.32	192.171	344.318	358.347	374.346	414.713	576.855
donorHB	Number of hydrogen bonds donated by the compound to water molecules in the medium.	0 – 6		0	2	1	4	0	1	1	4
accptHB	Number of hydrogen bonds accepted by the compound from water molecules in the medium.	2 – 20		5.25	6	4	11.75	5.25	6	1.7	10.2
#rotor	Number of rotatable bonds	0 – 15		0	6	2	10	5	6	7	13
PSA	Van der Waals surface area of polar nitrogen and oxygen atoms.	7 – 200		64.987	118.379	67.303	149.992	81.37	103.588	22.433	97.958

J. Mex. Chem. Soc. **2020**, *64*(4)
Regular Issue

ISSN-e 2594-0317

SASA	Total solvent accessible surface area (SASA) in Å^2 (probe radius 1.4 Å)	300 – 1000		465.275	625.373	379.584	541.771	611.822	613.269	774.588	945.34
Rule of Five	**Lipinski's rule of five** includes four descriptors for evaluating drug likeness • Mol_MW < 500 • Qplogpo/w < 5 • Donorhb ≤ 5 Accpthb ≤ 10.	The best drug- like compound does not violate any of these ranges	The rule was given number five as the descriptors' values are multiplets of 5	0	0	0	0	0	0	1	2
QPlogS	Predicted aqueous solubility, where S in mol/ dm^3 is the concentration of the solute in a saturated solution that is in equilibrium with the crystalline solid.	-6.0 – 0.5	**Oral absorption** prediction descriptors	-2.285	-4.503	-1.666	-1.433	-4.248	-4.297	-8.684	-7.225
CIQPlogS	Conformation-independent predicted aqueous solubility	-6.5 - 0.5		-2.76	-5.067	-2.203	-2.181	-5.207	-5.386	-7.033	-6.719
QPPCaco	Predicted apparent Caco-2 cell permeability in nm/sec. Caco2 cells are a model for the gut-blood barrier.	< 25 poor > 500 great		1896.224	240.239	937.285	66.861	2052.013	653.957	3381.617	279.696
HumanOral Absorption	Predicted qualitative human oral absorption	1 low 2 medium 3 high		3	3	3	2	3	3	3	3
Percent HumanOral Absorption	Predicted human oral absorption on 0 to 100% scale.	25 – 80 (more than 80 % is great)		95.908	83.841	85.727	55.142	100	94.541	100	74.699
Rule of Three	**Jorgensen's rule of three** including 3 descriptors for evaluating oral availability • Qplogs > -5.7 • QP pcaco > 22 nm/s • 1 ry Metabolites no < 7	The most orally available compound does not		0	0	0	0	0	0	1	1

J. Mex. Chem. Soc. **2020**, *64*(4)
Regular Issue

ISSN-e 2594-0317

		violate any of these ranges									
QPlogKhsa	Prediction of binding to human serum albumin	-1.5 – 1.5	**Plasma protein binding** prediction descriptors	-0.32	0.099	-0.496	-0.938	0.137	0.168	2.071	0.937
#metab	Number of likely metabolic reactions.	1 - 8	**Metabolism** prediction descriptors	1	6	2	6	5	6	3	6
QPlogPo/w	Predicted octanol/water partition coefficient	-2.0 – 6.5	**Excretion** prediction descriptors	1.758	2.44	0.955	-0.763	3.508	2.938	7.61	5.103
QPpolrz	Predicted polarizability ($Å^3$)	13 – 70		27.854	34.891	18.681	27.592	35.672	35.065	48.839	60.034
QPlogPC16	Predicted hexadecane/gas partition coefficient	4 – 18		7.061	11.201	6.284	10.503	10.077	10.469	12.719	17.642
QPlogPoct	Predicted octanol/gas partition coefficient	8 – 35		12.368	17.744	9.916	21.923	14.891	16.587	17.903	31.21
QPlogPw	Predicted water/gas partition coefficient	4 – 45		6.525	11.228	7.573	18.239	7.037	9.067	3.713	16.182
QPlogHERG	Predicted IC_{50} value for HERG K+ channels blockage	Not below -5.0	**Cardiotoxicity** prediction descriptors	-2.624	-5.513	-3.771	-3.683	-5.149	-4.865	-4.736	-5.216